The potential use of electrospun PLA nanofibres as alternative reinforcements in an epoxy composite system

Yu Dong [a,*], Tariq Mosaval [a], Hazim J. Haroosh [b], Rehan Umer[c], Hitoshi Takagi[d], Kin-Tak Lau[e]

[a] *Department of Mechanical Engineering, Curtin University, Perth, WA 6845, Australia*
[b] *Department of Chemical Engineering, Curtin University, Perth, WA 6845, Australia*
[c] *Department of Aerospace Engineering, Khalifa University of Science Technology & Research, Abu Dhabi 127788, United Arab Emirates*
[d] *Advanced Materials Division, Institute of Technology and Science, The University of Tokushima, Tokushima 770-8506, Japan*
[e] *Department of Mechanical Engineering, The Hong Kong Polytechnic University, Hung Hom, Kowloon, Hong Kong, China*

ABSTRACT

This pilot study elaborates the development of novel epoxy/electrospun polylactic acid (PLA) nanofibre composites at the fibre contents of 3, 5 and 10 wt% to evaluate their mechanical and thermal properties using flexural tests and differential scanning calorimetry (DSC). The flexural moduli of composites increase remarkably by 50.8% and 24.0% for 5 wt% and 10 wt% fibre contents, respectively, relative to that of neat epoxy. Furthermore, the similar tendency is also shown for corresponding flexural strengths being enhanced by 31.6% and 4.8%. Fractured surface morphology with scanning electron microscopy (SEM) confirms a full permeation of cured epoxy matrix into nanofibre structures and existence of non-destructive fibrous networks inside large void cavities. The glass transition temperature (T_g) of composites increases up to 54-60°C due to embedded electrospun nanofibres compared to 50°C for that of epoxy, indicating that fibrous networks may further restrict the intermolecular mobility of matrix in thermal effects.

KEYWORDS: biopolymers; electrospinning; fibres; mechanical properties; nanocomposites

* Corresponding author. Tel.: +61 8 92669055; fax: +61 8 92662681.
E-mail address: Y.Dong@curtin.edu.au (Y. Dong).

INTRODUCTION

The process of electrospinning[1-8] is relatively new and versatile to produce micro/nanofibre mats by means of simple experimental setup, which mainly consists of a syringe pump, a high voltage power supply, a solution-contained syringe attached with a metallic needle, as well as a collector (e.g. a rotating drum or a stand-alone mesh collector). The surface tension of solution is overcome by the electrostatic repulsive force in a high electric field. Hence the solution droplets with a uniform material flow are compelled to be stretched into fibrous structures in the direction of the collector.

The reinforcement effect of electrospun nanofibres [2,9] as potential nanofillers is of particular interest to materials scientists and engineers due to their high volume-to-weight ratio with large aspect ratios, efficient stress transfer to significantly enhance the stiffness and strength of nanocomposites, and attractive multifunctional properties. Even though some limited research work has concentrated on electrospun composite fibres [3,5,6,10] based on the direct composite fabrication in electrospinning, such study is still at an infant stage due to the common difficulty in good control of fibre quality arising from typical defects such as beads, internal pores, wavy and nonuniform fibres[2] for the robustness of fibre processing and property stability.

The early work was undertaken by Kim and Reneker[11] to evaluate the reinforcing effects of electrospun polybenzimidazole (PBI) nanofibres in both epoxy and rubber matrices. Such nanofibres toughened the brittle epoxy resin with higher fracture toughness and elastic moduli for 15 wt% nanofibre-reinforced epoxy composites as compared to those of composite counterparts with 17 wt% PBI fibrids. In the elastomeric matrix such as styrene-butadiene rubber (SBR), the Young's moduli and tear strengths of corresponding composites were also higher than those of pure SBR. Fong[12] attempted to use electrospun Nylon 6 fibres to reinforce the dental methacrylates of 2,2'-bis-[4-(methacryloxypropoxy)-phenyl]-propane

(Bis-GMA)/tri(ethylene glycol) dimethacrylate (TEGDMA). The mechanical properties of composites such as flexural strengths, elastic moduli, and work of fracture were all increased by 36, 26 and 42%, respectively, over those of neat resin with a small 5 wt% fibre content. Observed from the fracture surface, the cracks were deflected in the presence of Nylon 6 nanofibres. The interfacial bonding was required for the further improvement due to pull-out of Nylon 6 nanofibres from the matrix in the three-point bending tests. In the similar dental composite system, Tian et al.[13] also reported substantially higher mechanical properties of composites especially after being embedded with 1 wt% and 2 wt% Nylon 6/fibrillar silicate nanocomposite fibres. The silanised fibrillar silicate single crystals on the surface of nanofibres were detected to enhance the interfacial bonding between nanofibres and dental resin. Furthermore, Lin et al.[14] prepared electrospun polymer blends polyacrylonitrile (PAN)-poly (methyl methacrylates) (PMMA) nanofibre mats as core-shell structures to reinforce BIS-GMA. The PMMA chains entangled with the crosslinked dental resin network to create an *in situ* nanointerface formation in the shell structures for strong interfacial adhesion, thus resulting in the improvement of mechanical properties of composites when reinforced with 7.5 wt% PAN-PMMA nanofibres. Han et al.[15] fabricated poly(butylenes succinate) (PBS) reinforced with electrospun cellulose fibres that demonstrated a reinforcing effect due to the higher storage modulus of biocomposites than that of neat PBS. The uneven surfaces of cellulose fibres also suggested the good interfacial bonding occurred between cellulose fibres and PBS matrix.

Other electrospun polymer or composite fibres such as PAN fibres,[16] polystyrene (PS) fibres,[17] PAN/carbon nanotube composite fibres[18] and PAN/graphite nanoplatelet composite fibres[19] have also been studied systematically as good reinforcement candidates. However, according to our current knowledge from the available literature, electrospun polylactic acid (PLA) nanofibres have not been widely considered as the potential reinforcements though

PLA is regarded as one of popular biopolymers, extracted from natural plants/crops with enormous applications for medical science and engineering and bioproducts. This study aims to assess the feasibility of electrospun PLA nanofibres as new reinforcements to influence mechanical and thermal properties of epoxy/electrospun PLA nanofibre composites in stack laminate structures.

EXPERIMENTAL

Materials

PLA 3051D pellets with the density of 1.25 g/cm^3 for the purpose of injection or compression moulding and cosolvents of chloroform and methanol were supplied by Natureworks LLC, USA and Sigma-Aldrich Ltd, Australia, respectively. R180 low-viscosity epoxy resin (density: 1.15 g/cm^3 and viscosity: 110 cps) and H180 slow hardener (density: 0.95 g/cm^3 and viscosity: 80 cps) were obtained from Nuplex Composites, Australia. Such slow hardener with the pot life of 30-50 mins was selected to maximise the material handling time during which pouring and moulding processes of epoxy resin took place.

Electrospinning

To ensure the physical electrospinnability of PLA solution, PLA pellets were dissolved into chloroform and methanol cosolvents (volume ratio: 2:1) to achieve the PLA solution concentration at 7.5 wt%. About 3-mL PLA solution was loaded into the syringe that was mounted on a Fusion 100 syringe pump (Chemyx, Stafford, TX). The syringe pump was in operation at 3 mL/h to automatically purge the prepared solution. The high voltage setting was controlled by an ES30P-5W high voltage power supply (Gamma High Voltage Research, Ormond Beach, FL) at 25 kV. The fabricated fibre mats were finally collected from a stand-alone mesh collector covered with aluminium foils. A 20G metallic needle with the inner diameter about 0.584 mm was attached to the syringe, and the needle-to-collector distance was kept at 12 cm.

Fabrication of composite laminates

The prepared fibre mats (average thickness: 6.70-11.63 μm) were cut into strip-like sheets, peeled off from aluminium foils, and then stacked upon each other to form multilayered sheets. Epoxy/electrospun PLA nanofibre composites were manufactured at the fibre contents of 3, 5 and 10 wt%, which were calculated based upon the simple assumption that each PLA sheet has the uniform thickness without interlayer gaps with an average 75% porosity.[20] According to the material supplier's recommendation, epoxy resin and hardener at a fixed mix ratio of 5:1 were measured separately in two beakers, and then carefully added together and stirred inside a resealable plastic bag. Air bubbles generated during the stirring process were removed by using an ultrasonicating bath. The invoked disruptive wave in the bath disturbed the mixture and thus allowed the bubbles to be agitated towards the top surface of mixture liquid for further removal. A cast iron mould, assembled by top, middle and base plates, with a rectangular strip-like cavity of 100×40×2 mm^3 was used in the subsequent solution casting process. The epoxy mixture was initially poured onto the bottom half of the cavity to form an epoxy layer on which the stacked sheets were then carefully laid. The top plate with the same cavity was placed onto the sheets and fully tightened by screws. The rest of epoxy mixture was poured on the top surface of stacked sheets, resulting in the formation of the second epoxy layer. Acetate sheets were then positioned on the second epoxy layer to achieve good surface finish. A few light mass bars were used on the top of acetate sheets to assist in the impregnation of epoxy resin into porous fibre mats. The composite laminates inside the mould were initially cured in a vacuum oven at ambient temperature of 26 °C for about 18 h. After the demoulding step, full curing took place over a further 24-h period. Then they were polished with a MINITECH 263 polisher, PRESI, France and cut into rectangular testing samples with the dimensions of 40×10×2 mm^3. The key steps for the fabrication process are explicitly illustrated in Figure 1.

Testing and characterisation

The flexural tests were conducted using a 3-point bending rig mounted on an INSTRON 1196 frame 5500 series universal testing machine (load cell capacity: 500 N). At least three testing samples for each material batch were used, subjected to a crosshead speed of 8.53 mm/min with a support span of 32 mm.

The surface morphology of electrospun PLA nanofibre mats and composite bulk samples was examined by an EVO 40XVP scanning electron microscope, Germany at an accelerating voltage of 15 kV. All materials were sputter-coated with platinum at the initial sample preparation stage to provide the enhanced conductivity for better image contrast.

The differential scanning calorimetry (DSC) thermal analysis was undertaken with the aid of a PerkinElmer DSC 6000 from 25°C to 200°C at a scan rate of 10°C/min under the two heating-cooling cycle program. The DSC samples also underwent the isothermal condition at 200°C for 10 mins to remove any thermal history. The effect of fibre content on the glass transition temperature (T_g) was directly analysed from the first heating cycle.

RESULTS AND DISCUSSION

Flexural properties

Typical flexural stress vs. flexural strain curves are depicted in Figure 2(a), which suggests that with increasing the fibre content from 0 to 10 wt%, epoxy/electrospun PLA nanofibre composites become more brittle due to reduced flexural strains at break. As observed from Figure 2(b), the flexural moduli of composites initially decline at the fibre content of 3 wt%, further reach the maximum level of 2.76 GPa (50.8% increase relative to that of neat epoxy) at 5 wt%, and finally decrease moderately to 2.27 GPa (24.0% increase accordingly) at 10 wt%. The flexural strengths resemble the modulus trend with the maximum flexural strength of 102.78 MPa taking place at the fibre content of 5 wt% as well. This results in the increase of flexural strength by 31.6% as compared to that of neat epoxy. It can be confirmed that

electrospun PLA nanofibres play an important role as the effective reinforcements, especially at the fibre content of 5 wt%, which may be regarded as the optimum level in the material selection.

SEM evaluation

As seen from Figure 3(a), electrospun PLA nanofibre mats display the randomly oriented networks with the average fibre diameters ranging from 400-1000 nm. Neat epoxy has a brittle fracture with some extent of surface roughness, Figure 3(b). This roughness level was found to be enhanced in epoxy/electrospun PLA nanofibre composites presented in Figures 3(c)-(e), which may provide good resistance to the applied force during breaking (i.e. the deflection of cracks) due to the embedded nanofibres as indicated elsewhere.[13] In particular, based on the use of stack lamination process, a distinguishable interface exists between the epoxy-rich region (bottom-right side) and epoxy-embedded PLA nanofibre area (top-left side) in Figure 3(c). It appears that most of epoxy matrices have penetrated into the porous area of PLA nanofibre networks despite the difficulty in identifying the fibrous networks from the epoxy. Epoxy resin was previously reported to be a good compatibiliser in melt compounding process to increase the interfacial adhesion of polymer blends and thus improve their mechanical properties.[21-23] Even though our composites were prepared at room temperature, the heat dissipation during the epoxy curing stage may moderately accelerate the reaction between epoxy group with the terminal functional groups of neighbouring PLA such as hydroxyl or carboxyl groups,[21] thus resulting in the greatly enhanced interfacial adhesion. As normally a small amount of epoxy resin between 3-6 wt%[23] is required to work as a compatibiliser, the majority of epoxy matrices may not be affected by such a chemical reaction. As a result, the improved flexural strengths illustrated in Figure 2(b) can be attributed to the formation of strong interfacial bonding between electrospun PLA fibres and a small portion of effective epoxy compatibiliser. However, some local large voids over 60

μm in the lateral dimension, owing to the trapped air bubbles to form such manufacturing defects, were observed in all composite materials. As expected, these microsized voids may easily generate the weak fracture zones prone to the failure damage. Quite interestingly, fibrous networks are really manifested inside those large voids, Figures 3(d) and (e). This finding corroborates nondestructive fibrous structures still occur in the composite morphology. The constructed fibrous networks by connecting with the internal walls of void surfaces may, to a certain extent, alleviate the potential stress failure, which is anticipated to be under investigation in the future work. Most of these entangled fibrous networks seem to be well-bonded and interconnected, Figure 3(f). Nevertheless, a certain sign of partial fibre breakage still arises within the networks from the "fibre necking" effect, Figure 3(g). It is quite convincing that aforementioned chemical reaction may have minor destructive effect on the electrospun PLA fibrous networks. Meniscuses at the interfacial regions [highlighted using circles in Fig. 3(g)] between PLA nanofibres and epoxy matrices suggest relatively good wettability of their composites, and there is no evident interfacial fibre debonding or fibre fracture taking place.

DSC thermal analysis

The DSC results of epoxy/electrospun PLA nanofibre composites along with their typical T_g values are displayed in Figure 4. It can be seen evidently that embedded electrospun nanofibres give rise to the increase of T_g values of composites all above that of neat PLA at 50.05°C. Admittedly, with increasing the fibre content from 3 to 10 wt%, their T_g values simultaneously demonstrate a decreasing tendency from 59.64 °C to 53.5°C. The addition of PLA nanofibres is believed to constrain intermolecular mobility of epoxy matrix at elevated temperatures, which can be explained by trapping the epoxy molecules in their porous areas to form a very tight binding, as observed in Figure 3(c). As a consequence, T_g values have to

be increased up to a higher level in order to provide the good mobility of molecular chains in response to such thermal effects.

CONCLUSIONS

This study used a stack lamination method to successfully prepare novel epoxy/electrospun PLA nanofibre composites. The effective reinforcement of electrospun PLA nanofibres can be clearly confirmed with the maximum flexural modulus and strength increases of 50.8% and 31.6%, determined at the optimum fibre content of 5 wt%. Notwithstanding apparent large voids in connection with the internal well-bonded fibrous networks as well as localised partial fibre breakage take place, the SEM results still present a strong interfacial bonding between the PLA nanofibres and epoxy matrix. The additional electrospun PLA nanofibres are also shown to be effective fillers for the mobility restriction of epoxy molecules due to the increased T_g values.

REFERENCES AND NOTES

1 Y. Dzenis, *Science* **2004**, *304*, 1917-1919.

2 Z. M. Huang, Y. Z. Zhang, M. Kotaki, S. Ramakrishna, *Compos. Sci. Technol.* **2003**, *63*, 2223-2253.

3 Y. Dong, D. Chaudhary, H. Haroosh, T. Bickford, *J. Mater. Sci.* **2011**, *46*, 6148-6153.

4 H. J. Haroosh, D. S. Chaudhary, Y. Dong, *J. Appl. Polym. Sci.* **2012**, *124*, 3930-3939.

5 H. J. Haroosh, Y. Dong, D. S. Chaudhary, G. D. Ingram, S. Yusa, *Appl. Phys. A-Mater. Sci. Process.* **2013**, *110*, 433-442.

6 Y. Dong, T. Bickford, H. J. Haroosh, K. T. Lau, H. Takagi, *Appl. Phys. A-Mater. Sci. Process.* **2013**, *112*, 747-757.

7 N. N. Azman, S. Siddiqui, H. Haroosh, H. Albertran, B. Johannessen, Y. Dong, I. M. Low, *J. Synchroton Rad.* **2013**, *20*, 741-748.

8 H. J. Haroosh, Y. Dong, G. D. Ingram, *J. Polym. Sci. Part B-Polym. Phys.* **2013**, *51*, 1607-1617.

9 M. M. Bergshoef, G. J. Vancso, *Adv. Mater.* **1999**, *16*, 1362-1365.

10 K. M. Sawicka, P. Gouma, *J. Nanopart. Res.* **2006**, *8*, 769-781.

11 J. S. Kim, D. H. Reneker, *Polym. Compos.* **1999**, *20*,124-131.

12 H. Fong, *Polymer* **2004**, *45*, 2427-2432.

13 M. Tian, Y. Gao, Y. Liu, Y. Liao, R. Xu, N. E. Hedin, H. Fong, *Polymer* **2007**, *48*, 2720-2728.

14 S. Lin, Q. Cai, J. Ji, G. Sui, Y. Yu, X. Yang, Q. Ma, Y. Wei, X. Deng, *Compos. Sci. Technol.* **2008**, *68*, 3322-3329.

15 S. O. Han, W. K. Son, J. H. Youk, W. H. Park, *J. Appl. Polym. Sci.* **2008**, *107*, 1954-1959.

16 S. F. Fennessey, R. J. Farris, *Polymer* **2004**, *45*, 4217-4225.

17 K. H. Lee, H. Y. Kim, H. J. Bang, Y. H. Jung, S. G. Lee, *Polymer* **2003**, *44*, 4029-4034.

18 H. Ye, H. Lam, N. Titchenal, Y. Gogotsi, F. Ko, *Appl. Phys. Lett.* **2004**, *85*, 1775-1777.

19 J. J. Mack, L. M. Viculis, A. Ali, R. Luoh, G. Yang, H. T. Hahn, F. K. Ko, R. B. Kaner, *Adv. Mater.* **2005**, *17*, 77-80.

20 S. D. Mccullen, D. R. Stevens, W. A. Roberts, L. Clarke, S. H. Bernacki, R. E. Gorga, E. G. Loboa, *Int. J. Nanomed.* **2007**, *2*, 253-263.

21 F. C. Pai, S. M. Lai, H. H. Chu, *J. Appl. Polym. Sci.* **2013**, *130*, 2563-2571.

22 Y. Huang, Y. Liu, C. Zhao, *J. Appl. Polym. Sci.* **1998**, *69*, 1505-1515.

23 J. An, J. Ge, Y. Liu, *J. Appl. Polym. Sci.* **1996**, *60*, 1803-1810.

LIST OF FIGURES

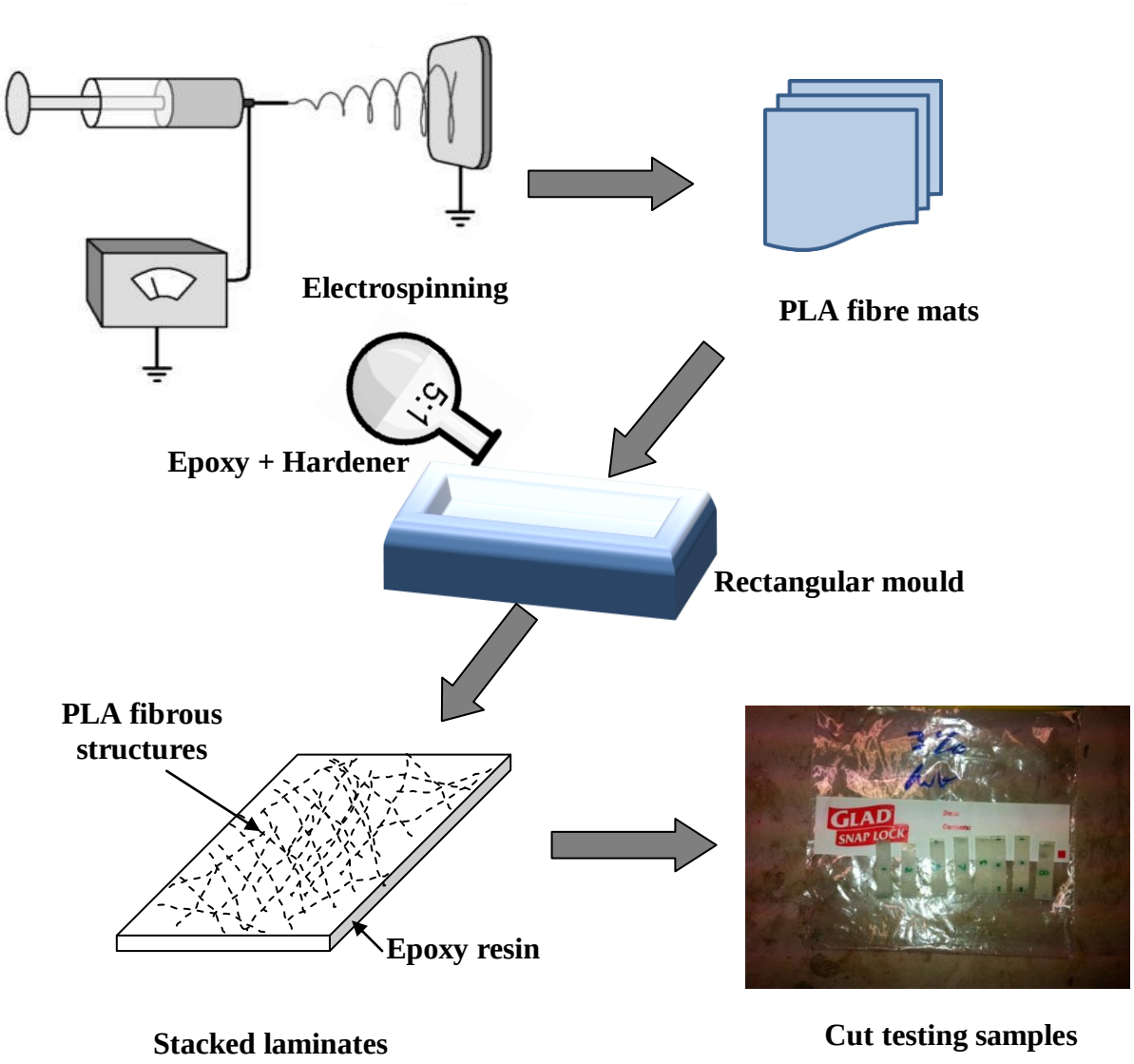
Electrospinning
PLA fibre mats
5:1
Epoxy + Hardener
Rectangular mould
PLA fibrous structures
Epoxy resin
Stacked laminates
GLAD
SNAP LOCK
Cut testing samples

FIGURE 1

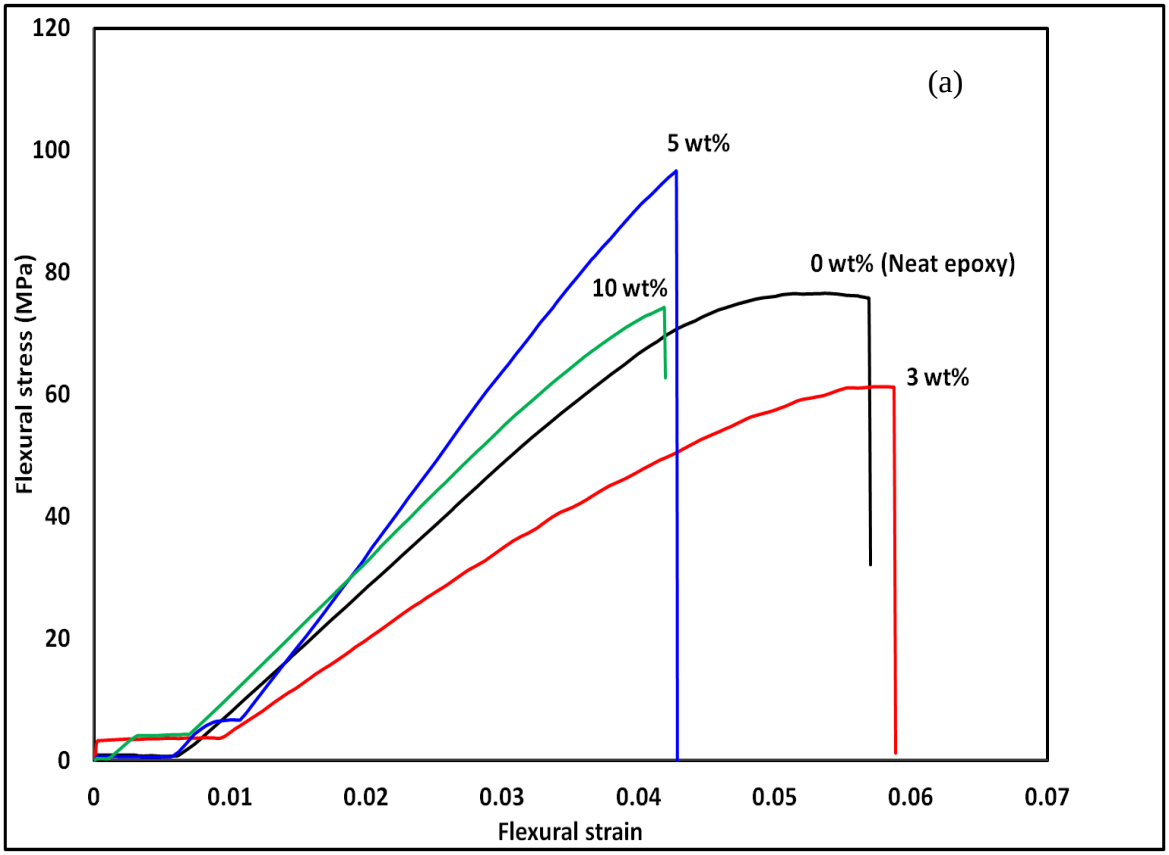
(a)
5 wt%
0 wt% (Neat epoxy)
10 wt%
3 wt%
Flexural stress (MPa)
Flexural strain
120
100
80
60
40
20
0
0
0.01
0.02
0.03
0.04
0.05
0.06
0.07

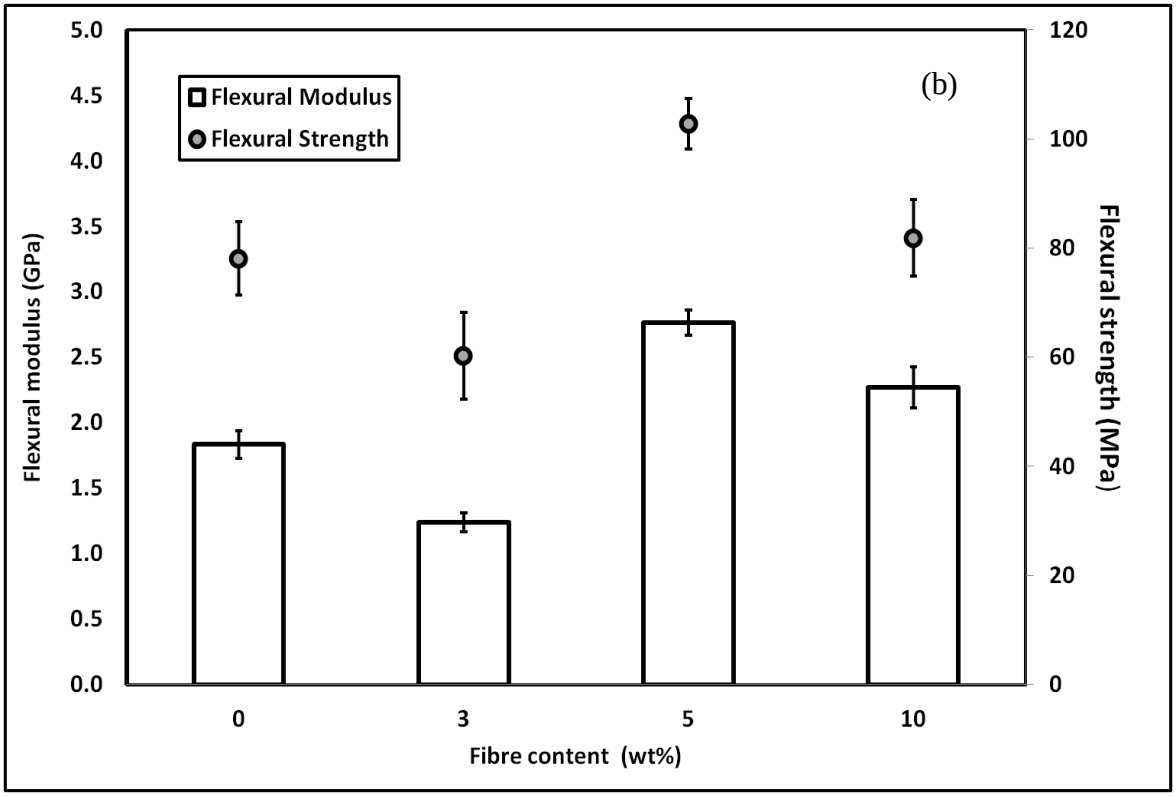
(b)
Flexural Modulus
Flexural Strength
Flexural modulus (GPa)
Flexural strength (MPa)
Fibre content (wt%)
5.0
4.5
4.0
3.5
3.0
2.5
2.0
1.5
1.0
0.5
0.0
120
100
80
60
40
20
0
0
3
5
10

FIGURE 2

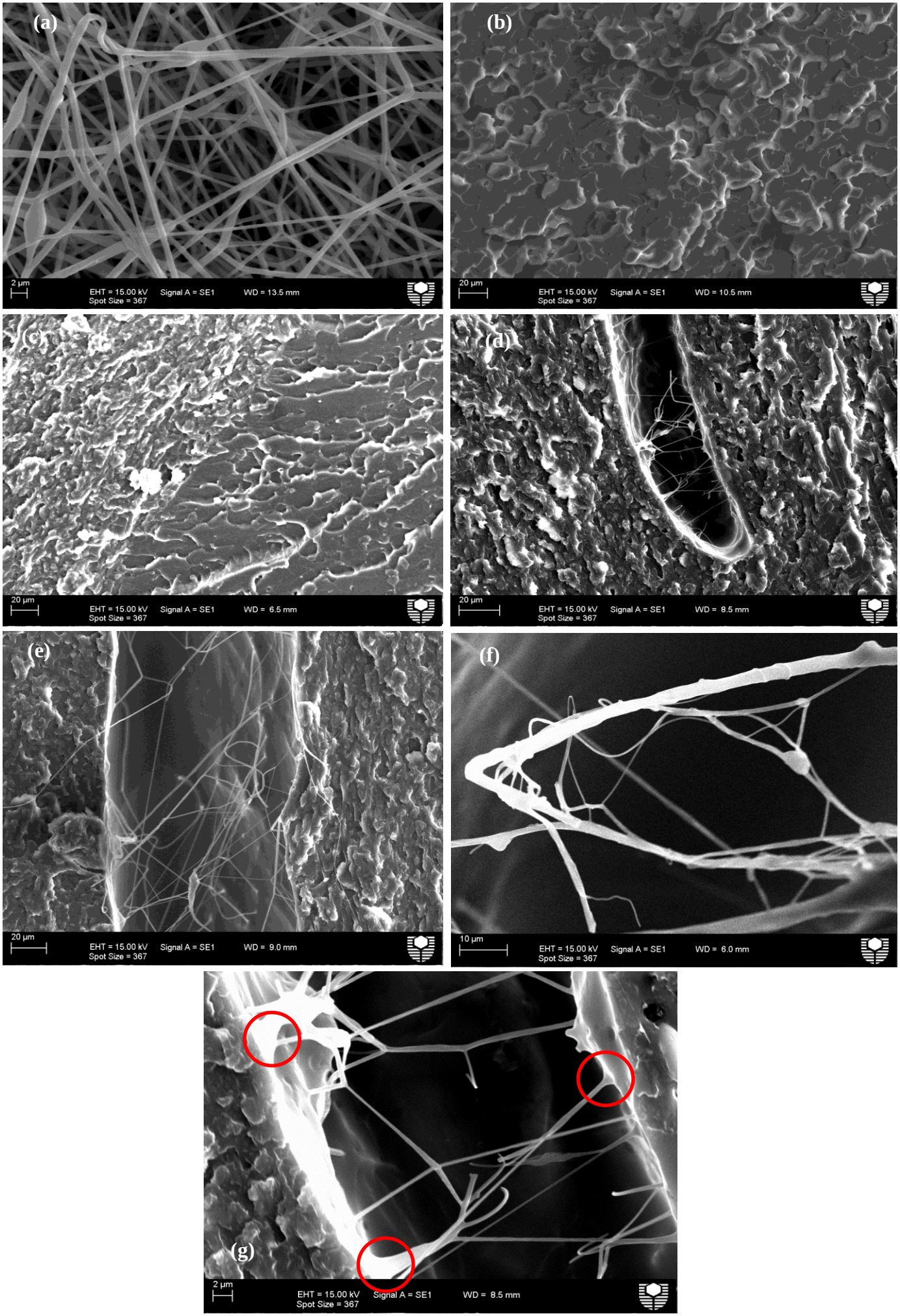
(a)
2 µm
EHT = 15.00 kV
Spot Size = 367
Signal A = SE1
WD = 13.5 mm
(b)
20 µm
EHT = 15.00 kV
Spot Size = 367
Signal A = SE1
WD = 10.5 mm
(c)
20 µm
EHT = 15.00 kV
Spot Size = 367
Signal A = SE1
WD = 6.5 mm
(d)
20 µm
EHT = 15.00 kV
Spot Size = 367
Signal A = SE1
WD = 8.5 mm
(e)
20 µm
EHT = 15.00 kV
Spot Size = 367
Signal A = SE1
WD = 9.0 mm
(f)
10 µm
EHT = 15.00 kV
Spot Size = 367
Signal A = SE1
WD = 6.0 mm
(g)
2 µm
EHT = 15.00 kV
Spot Size = 367
Signal A = SE1
WD = 8.5 mm

FIGURE 3

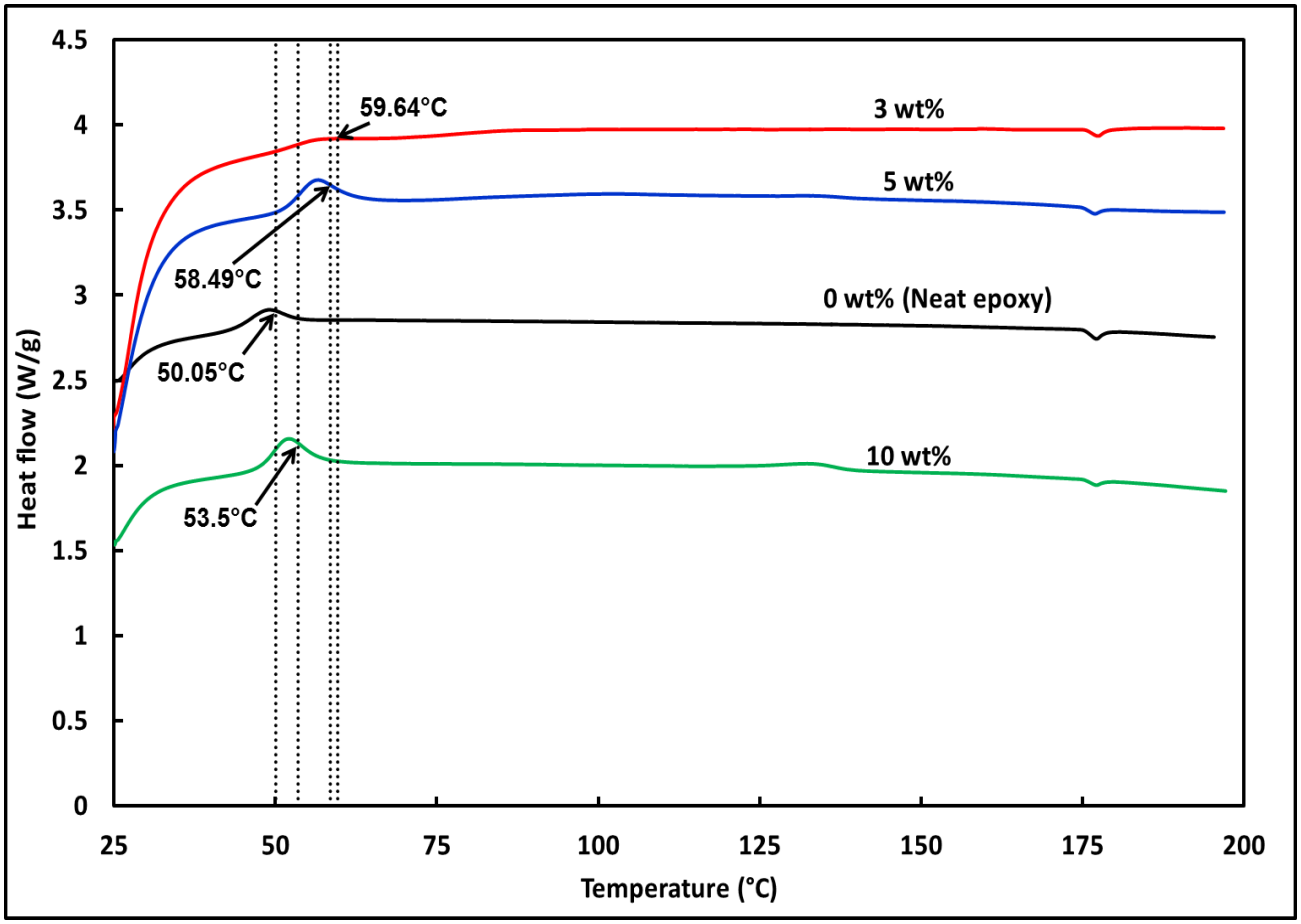
4.5
4
3.5
3
2.5
2
1.5
1
0.5
0
Heat flow (W/g)
25
50
75
100
125
150
175
200
Temperature (°C)
59.64°C
3 wt%
5 wt%
58.49°C
0 wt% (Neat epoxy)
50.05°C
10 wt%
53.5°C

FIGURE 4